

## Finite-field chiral tetracritical behavior in a distorted triangular antiferromagnet

M. L. Plumer and A. Caillé

*Centre de Recherche en Physique du Solide et Département de Physique, Université de Sherbrooke, Sherbrooke, Québec, Canada J1K 2R1*

(Received 28 October 1991)

The magnetic-field–temperature phase diagram of the antiferromagnetic planar model on a hexagonal lattice with a small basal-plane distortion is studied within mean-field theory. The convergence of four critical lines is shown to occur at a field  $H_x > 0$  as a consequence of in-plane anisotropy of the form  $Es_x^2$ . This is in contrast with the previously studied  $H = 0$  tetracritical behavior of the regular triangular lattice, as realized in  $\text{CsMnBr}_3$  [B. D. Gaulin *et al.*, Phys. Rev. Lett. **62**, 1380 (1989)]. The present system also exhibits the same chiral degeneracy and should be relevant to the previously misidentified multicritical behavior of  $(\text{CH}_3)_4\text{NMnCl}_3$ .

Tetracritical behavior exhibited by the antiferromagnetic planar model on a stacked triangular lattice is now reasonably well understood<sup>1–4</sup> with experimental realization found in  $\text{CsMnBr}_3$  (Refs. 5 and 6) [and possibly Ho (Ref. 7)]. The magnetic-field–temperature phase diagram (with  $H$  in the basal plane) shows two critical lines merging at the Néel temperature. Mean-field analysis<sup>2,8</sup> also reveals two additional critical lines merging at this point from the physically inaccessible region  $H^2 < 0$ . Thus, only two of the four critical lines can be observed experimentally in these systems. Additional interest in this behavior is due to the discrete chiral degeneracy associated with the frustration-induced  $120^\circ$  helical spin structure at  $H = 0$  and the suggestion of a new universality class.<sup>9</sup>

In the present work, mean-field results are given for the phase diagram associated with a slightly distorted (stacked) triangular lattice, which show a chiral tetracritical point at a finite  $H_x > 0$  due to a small in-plane anisotropy  $Es_x^2$ . Motivation for this study comes from the known structural phase transition that occurs in the planar antiferromagnet  $(\text{CH}_3)_4\text{NMnCl}_3$ , commonly referred to as TMMC. A small monoclinic ( $P2_1/b$ ) distortion<sup>10</sup> of the room-temperature hexagonal  $P6_3/m$  structure takes place at 128 K characterized by  $\gamma \cong 59.5^\circ$ . We suggest here that the previous characterization of the multicritical point in this material as  $n = 2$  bicritical<sup>11,12</sup> is not correct because of the frustration of the (nearly) triangular lattice. In addition to the in-plane spin anisotropy, such a distortion also gives rise to an asymmetry of the exchange interactions in the basal triangular plane. A consequence of such asymmetry is the stabilization of an incommensurate modulation with the interspin angle approximately  $120^\circ$  for small distortions.<sup>13</sup>

The magnetic properties of these distorted hexagonal antiferromagnets are characterized by the Hamiltonian<sup>11,12</sup>

$$\mathcal{H} = \frac{1}{2} \sum_{i,j} J_{ij} \mathbf{s}_i \cdot \mathbf{s}_j + D \sum_i s_{zi}^2 - E \sum_i s_{xi}^2 - \mathbf{H} \cdot \sum_i \mathbf{s}_i, \quad (1)$$

where  $\hat{\mathbf{z}} \parallel \hat{\mathbf{c}}$  and  $D, E > 0$  with  $D \gg E$ . We assume here that the anisotropy coefficient  $D$  is sufficiently large to en-

sure  $s_{zi} = 0$ . The only difference between (1) and the Hamiltonian that describes regular hexagonal crystals<sup>3</sup> is the in-plane anisotropy term  $E$ . The formulation of a suitable Landau-type free energy follows from our previous work.<sup>2,3,14</sup> To fourth order in the spin density

$$\mathbf{s}(\mathbf{r}) = \mathbf{m} + \mathbf{S} e^{i\mathbf{Q} \cdot \mathbf{r}} + \mathbf{S}^* e^{-i\mathbf{Q} \cdot \mathbf{r}}, \quad (2)$$

the result can be expressed as

$$\begin{aligned} F = & A_Q S^2 - A_x |S_x|^2 + B_1 S^4 + \frac{1}{2} B_2 |\mathbf{S} \cdot \mathbf{S}|^2 \\ & + \frac{1}{2} \tilde{A}_0 m^2 - \frac{1}{2} A_{x0} m_x^2 + \frac{1}{4} B_3 m^4 \\ & + 2B_4 |\mathbf{m} \cdot \mathbf{S}|^2 + B_5 m^2 S^2 - \mathbf{m} \cdot \mathbf{H}, \end{aligned} \quad (3)$$

where  $S^2 = \mathbf{S} \cdot \mathbf{S}^*$  and  $A_Q = a(T - T_Q)$ . Landau-type symmetry arguments require that all coefficients be *a priori* independent to give a phenomenological model. This free energy can also be derived from the Hamiltonian (1) within the molecular-field approximation,<sup>3</sup> which yields the relations

$$T_Q = -j^2 J_Q / a, \quad A_x = A_{x0} = 2j^2 E, \quad \tilde{A}_0 = A_{Q=0},$$

and  $B_i = bT$ , where  $a, b$  are related to the angular momentum  $j$  through the Brillouin function.<sup>8</sup> With only close-neighbor interactions included, the Fourier transform of the exchange integral is given by

$$\begin{aligned} J_Q = & 2J_c \cos(Q_z c) \\ & + 2[J' \cos(Q_x a) + 2J \cos(\frac{1}{2} Q_x a) \cos(bQ_y)], \end{aligned} \quad (4)$$

where  $b = \sqrt{3}a/2$ ,  $J_c$  represents the interplane interaction and the two intraplane couplings ( $J' \cong J$  for small distortions) are defined precisely as in Ref. 13. With  $J_c, J, J' > 0$ , a modulation characterized by simple antiferromagnetic order along the  $c$  axis ( $Q_z = \pi/c$ ) and an incommensurate [nearly  $120^\circ$ , e.g.,  $Q_x \cong 4\pi/(3a)$ ,  $Q_y = 0$ ] structure in the basal plane is stabilized. The inclusion of a small nonlocal anisotropic interaction of the form  $\sum_{i,j} J_{ij}^z s_{zi} s_{zj}$  would result in temperature and magnetic-field dependence of the incommensurate wave vector. Note that within a molecular-field treatment of the Ham-

iltonian (1), anisotropy terms that are *fourth* order in the spin density do not appear in the free energy (3). Some effects of such terms on the magnetic phase diagram in the case of purely hexagonal antiferromagnets are considered in Ref. 1. (From the analysis given below, it can be seen that terms such as  $m_x^4$  and  $|S_x|^4$  serve merely to renormalize the coefficients of the existing isotropic terms by a small amount.)

The  $xy$ -spin free energy (3) has the same structure as the one previously analyzed by us for the Heisenberg case with axial anisotropy,<sup>14</sup> and for the same reasons (frustration), two continuous transitions also occur at  $H=0$  in the present model system. At high temperatures (just below the Néel point), where  $S^2$  is small, the polarization of  $\mathbf{S}$  is determined by the second-order anisotropy term  $A_x$  to give a configuration  $\mathbf{S} \parallel \hat{x}$ . At lower temperatures, the fourth-order term  $|\mathbf{S} \cdot \mathbf{S}|^2$  is minimized by a helical polarization,<sup>15</sup>  $\mathbf{S} \cdot \mathbf{S} = 0$ , for  $B_2 > 0$ . This competition between these two terms then yields an elliptical configuration of the spin density at low  $T$ . Following the analysis of Ref. 14, the polarization vector can be written as

$$\mathbf{S} = S(\hat{x} \cos\beta + i\hat{y} \sin\beta) \quad (5)$$

and with  $\mathbf{H} \parallel \hat{x}$ , the free energy (3) becomes

$$F = A_0 S^2 + \frac{1}{2} B S^4 + \frac{1}{2} A_0 m^2 + \frac{1}{4} B_3 m^4 + B_5 m^2 S^2 - mH \\ + C_\beta S^2 \cos^2\beta + 2B_2 S^4 \cos^4\beta, \quad (6)$$

$$C_\beta = (A_x + 2B_2 S^2 - 2B_4 m^2)(4B_2 S^2), \quad (7)$$

where  $A_0 = \tilde{A}_0 - A_{x0} \equiv a(T - T_0)$  and  $B = 2B_1 + B_2$ . This free energy is minimized by the following values of the parameter, which characterizes the polarization vector:  $\beta = 0$  (phase 6), linear with  $\mathbf{S} \parallel \hat{x}$ ;  $\beta = \pi/2$  (phase 5), linear with  $\mathbf{S} \parallel \hat{y}$ ;  $0 < \beta < \pi/2$  (phase 7), elliptical with  $\mathbf{S} \perp \hat{z}$ . In addition, the paramagnetic state is described by  $S = 0$  (phase 1). (This numerical labeling of the phases follows our notation of Ref. 1.) At  $H = 0$ , the Néel temperature (1-6 transition) is given by  $T_{N1} = T_Q + A_x/a$ . As the temperature is lowered, a second transition (6-7) occurs to the elliptical phase at  $T_{N2} = T_{N1} - A_x B / (2aB_2)$ .

The schematic phase diagram for  $\mathbf{H} \parallel \hat{x}$  shown in Fig. 1(a) (based on calculations assuming  $B_i > 0$ ) can be understood with simple arguments. For sufficiently large field strengths, the anisotropy coefficient  $C_\beta$  can change sign so that the linear phase 5 with  $\mathbf{S} \perp \mathbf{H}$  is stabilized. The multicritical point occurs when the system becomes isotropic,  $C_\beta = 0$ , at the critical value of temperature and field ( $T_m, H_m$ ) as given in Ref. 14 (with  $A_z$  replaced by  $A_x$ ; note that the multicritical point of Ref. 14 is different from the present case, involving a spin-flop transition). Analytic expressions for the 1-5 and 1-6 phase boundaries are given by Eqs. (14) and (15), respectively, of Ref. 14. No competition is induced by a field  $\mathbf{H} \parallel \hat{y}$  so that the phase diagram as depicted in Fig. 1(b) occurs (with similar results for  $\mathbf{H} \parallel \hat{z}$ ).

The multicritical point of Fig. 1(a) has precisely the same symmetry and characteristics as the  $H = 0$  transition in  $\text{CsMnBr}_3$ ,<sup>2-6,8</sup> and can thus be described as an  $n = 2$  chiral tetracritical point. It occurs here at a finite

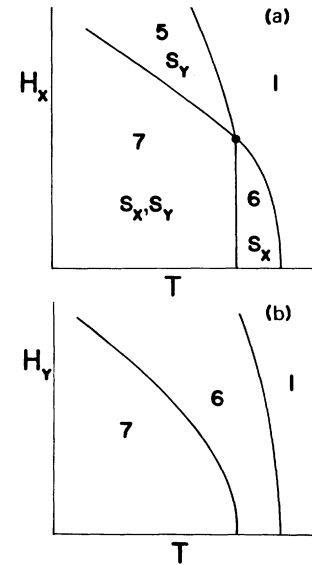


FIG. 1. Schematic phase diagrams for  $\mathbf{H}$  parallel (a) and perpendicular (b) to the easy in-plane axis showing the paramagnetic phases 1, linear phases 5 and 6, and elliptical phase 7. All lines represent continuous transitions. The solid circle in (a) denotes the chiral tetracritical point.

field  $H_m > 0$  as a consequence of the in-plane anisotropy  $A_x$ . An analogous situation can be found in the case of the unfrustrated (bipartite) planar (or Heisenberg) antiferromagnet when anisotropy is added. Only linear phases appear in this case since  $\mathbf{Q} = \frac{1}{2}\mathbf{G}$  (where  $\mathbf{G}$  is a reciprocal lattice vector) and the spin density is then independent of  $S_2$ . In the absence of anisotropy, a bicritical point occurs at  $H = 0, T = T_n$  in the  $(H^2, T)$  phase diagram, where  $\mathbf{S} \perp \mathbf{H}$  is stabilized at  $H^2 > 0$  and the configuration  $\mathbf{S} \parallel \mathbf{H}$  appears at  $H^2 < 0$ . The  $H = 0$  axis is a spin-flop line. Adding uniaxial anisotropy moves the multicritical point to a finite field  $H > 0$  and familiar  $n = 2$  ( $n = 3$ ) bicritical behavior is the result.<sup>16</sup>

There has been tremendous effort over the past 20 years to understand the low-temperature magnetic properties of TMMC.<sup>11,12</sup> This interest is largely due to the quasi-one-dimensional nature of the exchange interactions,  $J/J_c \sim 10^{-4}$  and the possibility for realistic quantitative comparison between experimental data and simple model calculations. The unusual magnetic-field dependence of the Néel temperature as well as anomalous spin excitations have been well explained by theories of soliton dynamics.<sup>11,17</sup> Of interest here is the cusplike behavior seen in the  $(\mathbf{H}, T)$  phase diagram for the paramagnetic boundary line with  $\mathbf{H} \perp \hat{z}$  (see Fig. 2). This feature phase has been attributed to the existence of a  $n = 2$  bicritical point<sup>11,12</sup> due to the anisotropy  $E$  (where the magnitude of  $E$  is about the same as the interchain exchange interaction  $J$ ). The first-order spin-flop line associated with this previously anticipated bicritical behavior, however, has not been observed but there appears to have been no systematic study of the phase diagram. Experimental difficulties are a consequence of the relatively low

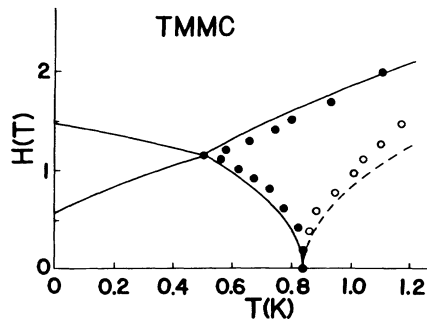


FIG. 2. Phase diagram of TMMC for  $H$  along the easy axis (solid circles form the data of Ref. 18 and solid lines from the fitted theory) and  $H$  perpendicular to the easy axis (open circles and dashed line). Experimental data is not available for temperatures below about 0.5 K. Phases are as indicated in Fig. 1.

temperatures involved, since the Néel temperature is 0.835 K and the apparent multicritical occurs at about 0.5 K. The effects of tripartite frustration have become better understood in recent years and it is clear from the analysis presented here that distorted hexagonal antiferromagnets described by the Hamiltonian (1), such as thought to be the case with TMMC, should exhibit  $n=2$  chiral tetracritical behavior and not a standard bicritical point.

The relevance of tetracritical behavior for TMMC can be further illustrated by the results of a crude fit of the theory to available experimental data,<sup>18</sup> in the spirit of Ref. 14. Although there are a large number of parameters [ $a$ ,  $T_0$ ,  $T_Q$ ,  $A_x$ ,  $B_i$  (where  $i=1-5$ )], some can be determined independently and the phase diagram is quite complicated. A comparison of paramagnetic susceptibility data<sup>19</sup> to the expression  $\chi_0^{-1}=a(T-T_0)$  yields the estimates  $a \cong 68$  (in cgs units per  $\text{cm}^3$ ) and  $T_0 \cong -90$  K. Extrapolation of the data of Ref. 18 for the 1-5 boundary to  $H=0$  gives  $T_Q \cong 0.16$  K and a fit to this data at  $T=1.1$  K then yields  $B_5 \cong -6.9$ . As with the quasi-one-dimensional system of Ref. 14, a negative value for  $B_5$  is responsible for the increase in temperature of the high-field phase boundary with increasing  $H$ . These results can then be used to obtain  $A_x \cong 45.9$ . With the assumption that the multicritical point occurs at  $T_m \cong 0.52$  K and  $H_m \cong 1.15$  T, the estimates  $B_3 \cong 24$  and  $B_4 \cong 6.9$  can be made.  $B_1$  and  $B_2$  (which are relevant only to the 5-7 and 6-7 boundary lines) cannot be estimated by fitting to the limited data available so the reasonable value (see Ref. 14) of 5.0 was assigned to both of these parameters.

The resulting phase diagram is shown in Fig. 2 for both  $H \parallel \hat{x}$  and  $H \parallel \hat{y}$ , along with the data of Ref. 18. The inability of the present mean-field model to yield good quanti-

tative agreement is not surprising in view of its omission of effects due to soliton dynamics. The results are of interest, however, as they offer a possible explanation for the experimental observation of only a single transition at  $H=0$  [compare with Fig. 1(a)], since a value  $T_{N2} < 0$  is predicted here in the case of TMMC. In addition, they provide some guidance for any future investigation of the low-temperature region of the phase diagram.

Additional complicating factors may be relevant in the case of TMMC regarding the existence of tetracritical behavior. Based on the assumption of a bipartite lattice, de Groot and de Jongh<sup>11</sup> suggest that a consequence of quasi-one-dimensional soliton dynamics may be the continuous reorientation of the spins ( $S_1$ ) as the field increases (with no spin-flop transition). The manifestation of this possibility for the real tripartite TMMC is likely the elimination of any true linear phase (except at  $T=0$ ) so that only the elliptical phase 7 would occur as an ordered state. In this case, the multicritical point of Figs. 1(a) and 2 would be replaced by a simple indentation in the paramagnetic boundary. Precisely this behavior would occur within the present model if an interaction of the form  $E' \sum_i s_{ix} s_{iy}$ , which is allowed by symmetry, were added to the Hamiltonian. Because the hexagonal lattice is only slightly distorted in TMMC, it can be expected that  $E'$  is very small. Only further experimental investigation can resolve these issues.

In conclusion, it has been demonstrated by this work that a slight distortion of the (stacked) triangular  $xy$  antiferromagnet moves the  $n=2$  chiral tetracritical point to a finite field  $H_m > 0$ . In contrast with systems of regular triangular symmetry (e.g.,  $\text{CsMnBr}_3$ ), the distortion allows for the possibility to observe all four critical lines. These results should be relevant to TMMC and isostructural  $(\text{CH}_3)_4\text{NMnBr}_3$  (TMMB, which has a much higher Néel temperature at 2.54 K).<sup>20</sup> The present study complements those of Ref. 9, which conclude that incommensurate in-plane order should occur as a consequence of such distortions. In spite of the strong interest in TMMC in recent decades, there appears to have been no neutron-diffraction determination of the magnetic structure in this material. It is of interest to note that chiral tetracritical behavior also occurs in the generalized version of Villain's fully frustrated  $XY$  model<sup>21</sup> and that the phase diagram of the hexagonal superconductor  $\text{UPT}_3$  exhibits a structure similar to that depicted in Fig. 1(a) as a consequence of coupling to long-range magnetic order.<sup>22</sup>

#### ACKNOWLEDGMENTS

This work was supported by Natural Sciences and Engineering Research Council (NSERC) of Canada and le Fonds Formation de Chercheurs et l'Aide à la Recherche (FCAR) du Québec.

<sup>1</sup>M. L. Plumer, A. Caillé, and K. Hood, Phys. Rev. B **39**, 4489 (1989).

<sup>2</sup>M. L. Plumer and A. Caillé, Phys. Rev. B **41**, 2543 (1990).

<sup>3</sup>M. L. Plumer and A. Caillé, Phys. Rev. B **42**, 10 388 (1990); J.

Appl. Phys. **69**, 6161 (1991).

<sup>4</sup>H. Kawamura, A. Caillé, and M. L. Plumer, Phys. Rev. B **41**, 4416 (1990).

<sup>5</sup>B. D. Gaulin, T. E. Mason, M. F. Collins, and J. Z. Larese,

- Phys. Rev. Lett. **62**, 1380 (1989).
- <sup>6</sup>M. Poirier, M. Castonguay, A. Caillé, and M. L. Plumer, Physica B **165&166**, 171 (1990); T. Goto, T. Inami, and Y. Ajiro, J. Phys. Soc. Jpn. **59**, 2328 (1990); T. E. Mason, C. V. Stager, B. D. Gaulin, and M. F. Collins, Phys. Rev. B **42**, 2715 (1990).
- <sup>7</sup>M. O. Steinitz, M. Kahrizi, and D. A. Tindall, Phys. Rev. B **36**, 783 (1987).
- <sup>8</sup>M. L. Plumer, A. Caillé, and H. Kawamura, Phys. Rev. B **44**, 4461 (1991).
- <sup>9</sup>H. Kawamura, Phys. Rev. B **38**, 4916 (1988); **42**, 2610(E) (1990); J. Phys. Soc. Jpn. **58**, 584 (1989).
- <sup>10</sup>M. T. Hutchings, G. Shirane, R. J. Birgeneau, and S. L. Holt, Phys. Rev. B **5**, 1999 (1972); Y. Milk and M. Couzi, J. Phys. C **15**, 6891 (1982); M. N. Braud *et al.*, J. Phys.: Condens. Matter **2**, 8209 (1990).
- <sup>11</sup>H. J. M. de Groot and L. J. de Jongh, Physica B **141**, 1 (1986).
- <sup>12</sup>J.-P. Renard, in *Organic and Inorganic Low-Dimensional Crystalline Materials*, edited by P. Delhaes and M. Drillon (Plenum, New York, 1987).
- <sup>13</sup>H. Kawamura, Prog. Theor. Phys. Suppl. **101**, 545 (1990); W. Zhang, W. M. Saslow, and M. Gabay, Phys. Rev. B **44**, 5129 (1991).
- <sup>14</sup>M. L. Plumer, K. Hood, and A. Caillé, Phys. Rev. Lett. **60**, 45, 1885(E) (1988).
- <sup>15</sup>M. B. Walker, Phys. Rev. B **22**, 1338 (1980).
- <sup>16</sup>M. E. Fisher, Phys. Rev. Lett. **34**, 1634 (1975).
- <sup>17</sup>J. A. Holyst and H. Benner, Solid State Commun. **79**, 703 (1991).
- <sup>18</sup>K. Takeda, T. Koike, T. Tonegawa, and I. Harada, J. Phys. Soc. Jpn. **48**, 1115 (1980).
- <sup>19</sup>R. Dingle, M. E. Lines, and S. L. Holt, Phys. Rev. **187**, 643 (1969); L. R. Walker, R. E. Dietz, K. Andres, and S. Darack, Solid State Commun. **11**, 593 (1972).
- <sup>20</sup>H. Tanaka *et al.*, J. Phys. Soc. Jpn. **55**, 2369 (1986); D. Visser and G. J. McIntyre, Physica B **156&157**, 259 (1989).
- <sup>21</sup>B. Berge, H. T. Diep, A. Ghazali, and P. Lallemand, Phys. Rev. B **34**, 3177 (1986); G. Parker, W. M. Saslow, and M. Gabay, *ibid.* **43**, 11 285 (1991).
- <sup>22</sup>See, e.g., R. Joynt, Europhys. Lett. **16**, 289 (1991).